Geotechnical Engineering in the XXI Century: Lessons learned and future challenges
N.P. López-Acosta et al. (Eds.)

doi:10.3233/STAL190359

CO_2 Geological Storage: Performance of Cement-Rock Interface

Juan Cruz BARRÍA[a], Diego MANZANAL[a,b,1] and Jean Michel PEREIRA[c]
[a]*Universidad Nacional de la Patagonia UNPSJB – CONICET, Argentina*
[b]*ETSICCyP, UPM (España)*
[c]*École des Ponts ParisTech, Lab Navier (UMR 8205 CNRS-IFSTTAR-ENPC), France*

Abstract: Geological storage of CO_2 in saline aquifers or depleted reservoirs requires establishing the degree of safety and efficiency of this storage operation. To do this, it is necessary to evaluate areas of weakness where CO_2 leakage could occur in the vicinity of the injection well. It is important to understand the chemical (C) and hydro (H)-mechanical (M) coupling (CHM) that occurs at the various interfaces of the well. This work focuses on the numerical analysis of the CHM coupling in the interface rock cover-cement ring with a finite element program. The numerical study includes identifying the components of the hardened cement paste through a formulation and its contribution to the CHM behavior of the same in the presence of CO_2. This formulation has been modified to incorporate additions of bacterial nanocellulose and glass microspheres. The results are presented as a function of changes in permeability, volumetric proportions molar quantities. The numerical study shows the advantage of the use of this type of tools for the study of possible real scenarios in CO_2 injection processes in deep wells.

Keywords. Interface cement-rock, chemo-hydro-mechanics coupling, nanopolymers, glass microsphere, geological storage.

1. Introduction

Carbon sequestration in abandoned oil fields, along with deep saline aquifer reservoirs and unminable coal beds, are being considered effective solutions for reducing CO_2 emissions to the atmosphere. These deposits permit to storage millions of m^3 of CO_2. An efficient reservoir for carbon sequestration is the one that has temperature just above the supercritical point and great pressures. These conditions allow to storage largest volumes of CO_2. (Supercritical state is reached at temperatures greater than 31.6°C and minimum pressures of 7.3 MPa).

The reservoir requires sufficient capacity and high porosity which would allow a good injectivity and a caprock with very low permeability to prevent CO_2 leakage through it. While drilling, the zone near the well is damaged and faults/fracture in cap rock could provide leakage paths of supercritical CO_2 ($scCO_2$) to upper environments, so is imperative preventing the escape of these gases through the preferential paths.

The cement glass G used in oil industry is chemically unstable against CO_2 and much less against $scCO_2$. The cement used during the completion of the new wells must withstand the attack of $scCO_2$. Experimental tests and numerical models are being

[1] Corresponding Author, d.manzanal@upm.es

development to study the behavior of the hardened cement paste at these conditions. New additives such as nanocellulose are being added to the mix to improve the cement properties [1].

The first step in the cement carbonation in oil abandoned field is the dissolution of CO_2 in water, which produces carbonic acid. Geochemical studies of cement paste show that advance of carbonic acid through cement paste produce principally the dissolution of portlandite CH (calcium hydroxide – $Ca(OH)_2(s)$) and C-S-H (calcium silicate hydrate), and the precipitation of calcium carbonate. The first reaction of carbonation in cement is the dissolution of CH:

$$CH + CO_2 \rightarrow CaCO_3 + H_2O \quad \text{(Simplified)} \tag{1}$$

The characteristic times of the chemical reactions are very small relative to the slow diffusion of ions in the in-pore fluid so the reactions can be assumed as instantaneous [2]. These chemical reactions induce changes of porosity and the mineral composition of the solid phase. After the dissolution of CH, the pH level is significantly reduced, allowing the second reaction that describes the carbonation of the C-S-H.

$$0.625\ CSH + CO_2 \rightarrow CaCO_3 + 1.3\ H_2O + 0.625\ SiO_2(H_2O)_{0.5} \quad \text{(Simplified)} \tag{2}$$

The formation of amorphous silica increases porosity and reduces structural integrity while the formation of $CaCO_3$ increases cement impermeability and compressive strength. This is only temporarily because $CaCO_3$ in a water acidified medium in presence of CO_2 prompts mineral dissolution. This dissolution continues until thermodynamic equilibrium is reached [3]. This last reaction causes the leaching of $CaCO_3$ which increases porosity, permeability and reduces compressive strength. The final result of the cement matrix is a porous medium with very low resistance, incapable to maintain wellbore integrity and sealing capacity.

The modification of cements to lower the density is a subject of interest in the cementing of wells. The objective is to modify the cement matrix, making it lighter but maintaining a high resistance and low permeability in its hardened state. Preliminary laboratory studies carried out at ITPN Laboratory (CONICET-UBA) by the authors (Martin 2017, Martin et al., 2017) show that an adequate combination of glass microspheres (GM) and bacterial nanocellulose (BNC) appear to achieve the desired objective, although a greater number of tests are required for confirmation.

2. Numerical modeling

The numerical code utilized is a coupled chemo-poromechanical model [2] implemented in BIL 2.3.0 finite element code [21] This code was written using the classic balance equations of continuum mechanical relative to mass, momentum, entropy and energy. The model assumed has 1D axisymmetry under plane strain conditions in the axial direction and C-S-H carbonation does not start until the portlandite is completely carbonated; because Portlandite maintains a high pH level (pH > 12). Chemical reactions (carbonation-dissolution) occurring in the system produce variation on the transport and mechanical properties in the system.

To demonstrate the initial operation of the program, we simulated the experiments of Barlet and Rimmelé [4]. In their experiment, they work with 1 inch-diameter x 2 inch samples made with conventional Portland cement class G with a w/c ratio of 0.44 using fresh water and additives following the API Specifications.

The present work analyzes the sample cured during 72 hours at 90 °C and 20.68 MPa and subsequently exposed to several days submerged in water saturated with $scCO_2$. Alteration front analysis shows a penetration approximately of 1 mm, 2 mm, 3 mm and 5 mm for 2 days, 4 days, 7 days and 21 days correspondingly.

3. Characteristics of the hydrated cement

3.1. Porosity

Porosity is very variable for cements, and depends mainly on the w/c ratio and the type of curing in which the specimen is placed. Some authors estimate porosities greater than 30% [4-7], while others approximate it from 20% to 30% [8-11]. Regardless of the kind of oil cement in question (G or H), it can be generalized that the porosities of oil cements are around 25% to 35%.

3.2. Intrinsic permeability

The intrinsic permeability is independent of the conditions to which a material is initially subjected. Since cement is a heterogeneous material, there is no unique intrinsic permeability value for cement. [12] in their experiments reports values of 1×10^{-16} m^2 to 1×10^{-20} m^2. This is supported by [9] and [13] where they obtain values in order of 1×10^{-19} m^2 y 1×10^{-20} m^2 and [11] calculates values after an excessive heating to the hardened cement paste in the order of 1×10^{-16} m^2, so it can be assumed that this order of magnitude is for fissured cements.

3.3. Diffusivity in cement

The diffusivity of cement for class G and H has also been variable for different authors. [14] performs a compilation of the different transport mechanisms of cement G subjected to an environment of $scCO_2$ and cites diffusivity values of 1×10^{-12} m^2s^{-1} up to 1×10^{-14} m^2s^{-1}. [13] gives an example of diffusion in the order of 1×10^{-12} m^2s^{-1} and [2] determines a value of 1×10^{-10} m^2s^{-1} on the simulation.

4. Initial volumetric proportions of hydrated cement

Hydrated Portland cement compounds are mainly C-S-H, $Ca(OH)_2$, and hydrated aluminates. The volumetric content of the aforementioned and the porosity depend substantially on the cement type, w/c ratio, hydration degrees and curing temperature. So, is necessary to estimate these proportions on for the simulation.

In some articles the amount of $Ca(OH)_2$ varies between 15 to 25% [9, 13], with commonly accepted values being percentages of 18 to 20% [2].

In particular, Class G and H cements have very low initial aluminates due to API requirements to be resistant to sulfate attack (C3A ≤ 3% and C4AF + 2 C3A ≤ 24%). So the hydrated components of aluminate have low percentage, around 8 to 14%. [2, 8, 16]. Finally, the most important phase of cement in terms of compressive resistance, phase C-S-H, can vary between 60 to 27% in volume fraction. [2, 16]

5. Transport parameters to calibrate.

The mesh used to represent the cement sample of the experiment is half of the sample (12.7mm), which allows studying the progress of carbonation from the outer surface to the core. It consists of 502 elements which have the cement properties.

The main parameters that influence the chemo-poromechanical behavior in addition to the initial values are the intrinsic permeability κ and the diffusion coefficient deff. The intrinsic permeability is linked to the initial porosity of the cement paste [17]. For this type of cement, it can be calculated by Eq. (3).

$$\kappa = \text{kappa0} * \left(\frac{\phi_F}{0.26}\right)^{11} * 10^{-19}\ \text{m}^2 \tag{3}$$

where ϕ_F = pore volume occupied by the pore fluid per unit volume of porous medium.

Being kappa0= Parameter to calibrate

While the diffusion coefficient is also affected by porosity as define Eq. (4):

$$d_{eff} = \text{diff0} * e^{(9{,}95\phi_F - 29{,}08)} \tag{4}$$

Being diff0= Parameter to calibrate.

These equations are empirical and do not exactly represent the transport phenomenon within the cement matrix. The parameters kappa0 and diff0 can be modified to obtain values of intrinsic permeability and diffusivity suitable for class G or H cements.

To obtain the diffusion and permeability parameters for this particular cement used by Barlet and Rimmelé to later be used in the simulation at reservoir level, porosity maintains the same experimental value of 32.5% for the first simulation. As the rest of volumetric proportions are variable, values were adopted from literature: C-S-H 40.5%, $Ca(OH)_2$ 18% and aluminates 9%. CO_2 concentration was calculated taking into account: water volume, temperature, pressures and mole fraction of CO_2 in water. The calculations show values of 1200 mol/m^3.

Table 1. Initial medium conditions for simulations.

η_{vis} [Medium viscosity] [MPa.s]	K_F [Medium compressibility] [MPa]	K_F [Medium density] [kg/m³]	R_c [Compressive strength] [MPa]	R_t [Tensile strength] [MPa]
0.5 10-9	1000	2200	45	4.5

Table 2. Molar Volumes [cm^3/mol].

ν^S_{CH}	$\nu^S_{C-S-H_{1.6}}$	$\nu^S_{CaCO_3}$	$\nu^S_{SiO_2(H_2O)_{0.5}}$	$\nu^F_{H_2O}$
33.1	84.7	36.9	31	18.85

A representative simulation under downhole conditions in the context of CO_2 geological storage was made to know the advance and properties of carbonation along time in cement. The well-system modeled consisted in a 2 cm cement annulus thickness under downhole conditions with a concentration of supercritical CO_2 of 1800 mol/m^3 like Figure 1. We used the same transport values after determining the permeability and diffusion parameters from the previous simulation.

A modification in the homogenization formulation was implemented adding the bacterial nanocellulose (BNC) and glass microspheres (GM) characteristics for a comparison between the usual Portland class G cement and the new cement.

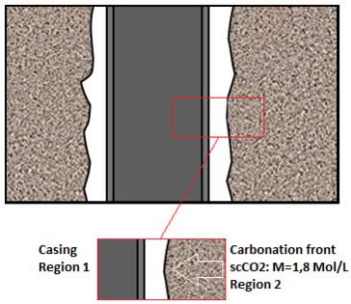

Figure 1. Well-system analyzed.

This modified cement contains the following proportions: porosity 28%, CH 14.07%, C-S-H 23.872%, Al 5%, BNC 0.058% and GM 29% and the medium conditions are the same as the previous simulation.

Table 3. Initial conditions for downhole simulation.

Inclusion	Volumetric prop. CP	Volumetric prop. CP-GM-BNC	Bulk modulus [GPa]	Shear modulus [GPa]
Porosity	0.325	0.28	-	-
CH	0.18	0.1407	33.00	14.50
C-S-H	0.405	0.23872	25.00	18.40
Aluminates	0.09	0.05	27.00	9.50
Calcite	0.00	0.00	69.00	37.40
GM	0.00	0.29	30.00	20.00
BNC	0.00	0.00058	27.778	9.259

6. Results and discussion

6.1. Experimental modeling.

In this section we present the sensitivity analysis of parameters to calibrate the numerical model in order to reproduce the experimental results of Barlet (2006). The case of storage of CO_2 in an oil well and the chemical-mechanical interaction are also analyzed. The comparison is made for conventional cements and modified cements with additions of bacterial nanocellulose and glass microspheres.

Table 4 and Table 5 shows values of the intrinsic permeability and diffusion coefficient varying kappa0 and diff0.

As it can be observed, the values of permeabilities and diffusivity are in the range of the admissible values for cements class G previously mentioned.

Table 4. Values of κ for different values of kappa0 and diff0.

Porosity	Parameter kappa0 [m²] K					
	0.1	**0.5**	**1**	**1.2**	**1.5**	**2**
0.325	1.1642E-19	5.8208E-19	1.16415E-18	1.397E-18	1.7462E-18	2.3283E-18

Table 5. Values of deff for different values of kappa0 and diff0.

Porosity	Parameter kappa0 [m²] K					
	0.1	**0.5**	**1**	**10**	**20**	**30**
0.325	5.9582E-13	2.9791E-12	5.9582E-12	5.95822E-11	1.1916E-10	1.7875E-10

Calibrating the model for kappa0=1.2 and diff0=20; a good representation of the carbonation front can be observed in Figure 2. Barlet approximates the carbonation front rounding to the millimeter. In our model, the carbonation is slightly ahead.

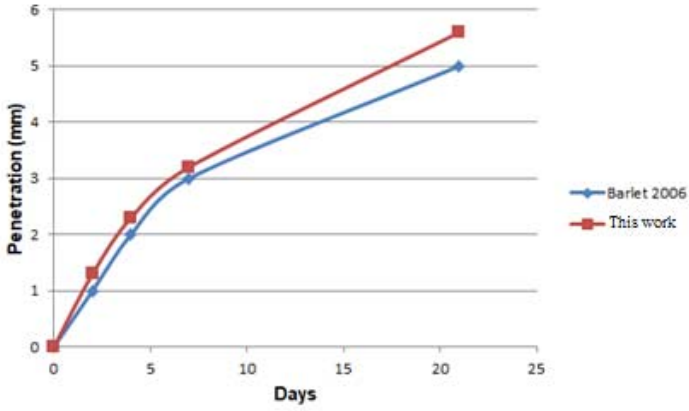

Figure 2. Comparison of the carbonation front between experimental and numerical modeling.

Additional characteristics on the variability of the carbonation front using these transport parameters can be approached; permeability (Figure 3) and volumetric proportions (Figure 4) variations along the sample. Carbonation advance forms calcite from CH and CSH, which grows inside the pores, this produce a reduction on the porosity and in consequence, a decrease in permeability that difficult the entry of more CO_2 into the cement matrix.

Formation of calcite increases in small scale the compressibility module. However, once the CH is depleted and the CSH carbonation starts, the total compressibility module decreases. The compressibility module of only calcite is less than the sum of the CH and CSH. In the volumetric proportions, porosity decreases and inert components increase when the calcite is formed. The penetration of calcite in the graphics starts with the CH area and continues to the CSH when there is no longer CH to consume (Figure 4).

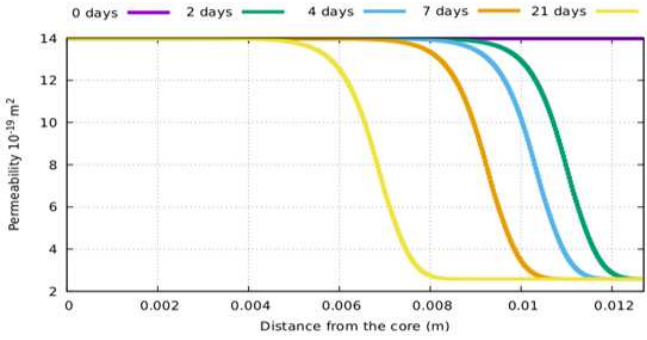

Figure 3. Permeability for kappa0=1,2 y diff0=20.

6.2. Well-system modeling.

Permeability is reduced by a factor of 10 and reaches values of 1×10^{-20} m^2. This increment in impermeability should diminish the future advance of carbonation front. However, the carbonation front seems to be approximately the same for both cements, proving in our model that diffusivity is the most important factor in the advancement of cement carbonation. A more detailed research of diffusivity in cement is required to confirm these results.

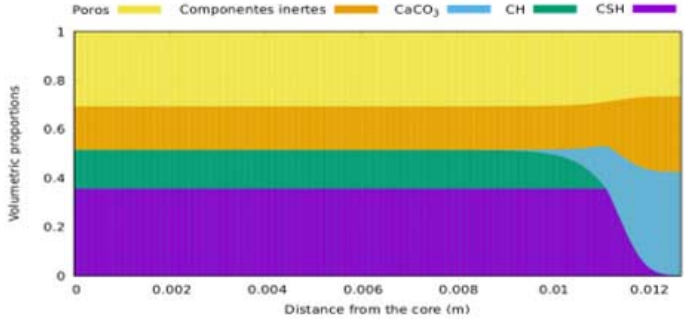

Figure 4. Volumetric proportions for kappa0=1,2 y diff0=20.

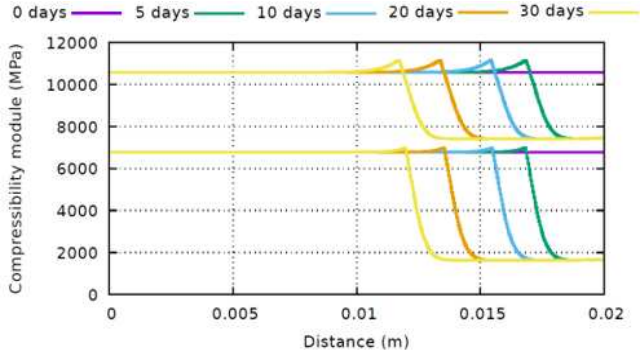

Figure 5. Compressibility module comparison between CP(Below) and CPGMBNC(Above).

With the addition of glass microspheres and nanocellulose we achieve a lighter cement to be used. Another benefit is the resistance. We can see this on the increase of the compressibility module, reaching values of 7500 MPa for the modified cement and only 1800 MPa for the common cement (Figure 5).

Carbonation products are less in the modified cement due to the fewer amount of CH and CSH that can be consumed by the H2CO3 (Figure 6). Smaller porosity, fewer amount of products to be consumed, lighter and resistant mixtures are sought properties for cements in the context of CO_2 geological storage.

7. Conclusion

A chemo-poro-mechanical model of $scCO_2$ attack on a cement annulus in an abandoned oil well in the context of CO_2 storage is presented. A modification on the formulation is implemented to add the nanocellulose and glass microsphere characteristics such as bulk and shear modulus. A comparison between experimental and simulation is analyzed to determine the properties of the cement used. Once known these properties, a simulation under downhole condition in the context of CO_2 geological storage is represented.

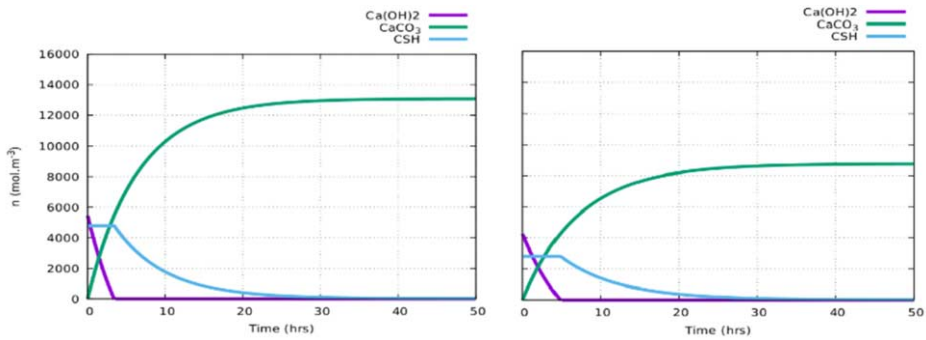

Figure 6. Molar quantities comparison between CP(Left) and CPGMBNC(Right).

Results shows a decrease of permeability and carbonation products in the modified cement and also an increase in compressibility modulus, demonstrating an improvement in the characteristics for the use of this cement in oil industry for a future EOR recovering with CO_2 gas or CO_2 geological storage.

In these results, the model demonstrates a good precision in data, so it can be implemented to different systems under different established conditions. However, more examples should be run on different and conditions to improve the program.

In the case described in the article, the modified cement contains nanocellulose and glass microspheres. To better characterize the nanocellulose, laboratory tests are being carried out, exposing the modified cement with only nanocellulose to $scCO_2$ and simulations are underway to have a better understanding of the behavior of cement against $scCO_2$.

References

[1] X. Sun, Q. Wu, S. Lee, Y. Qing, and Y. Wu, "Cellulose Nanofibers as a Modifier for Rheology, Curing and Mechanical Performance of Oil Well Cement," Sci. Rep., vol. 6, pp. 1–9, 2016.

[2] V. Vallin, J. M. Pereira, A. Fabbri, and H. Wong, "Numerical modelling of the hydro-chemo-mechanical behaviour of geomaterials in the context of CO 2 injection,", 2013.

[3] S. Kim and J. C. Santamarina, "Reactive fl uid fl ow in CO 2 storage reservoirs : A 2-D pore network," vol. 473, pp. 462–473, 2015.

[4] G. Rimmelé, V. Barlet-gouédard, O. Porcherie, B. Goffé, and F. Brunet, "Cement and Concrete Research Heterogeneous porosity distribution in Portland cement exposed to CO2-rich fluids" 2008.

[5] A. Materials, "Reduction of set cement permeability in oil well to decrease the pollution of receptive environment using spherical nanosilica," vol. 6, pp. 101–104, 2011.

[6] K. J. Krakowiak, J. J. Thomas, S. Musso, S. James, A. Akono, and F. Ulm, "Cement and Concrete Research Nano-chemo-mechanical signature of conventional oil-well cement systems : Effects of elevated temperature and curing time," Cem. Concr. Res., vol. 67, pp. 103–121, 2015.

[7] G. Rimmelé, B. Goffé, and O. Porcherie, "Well Technologies for CO 2 Geological Storage : CO 2 - Resistant Cement," vol. 62, no. 3, pp. 325–334, 2007.

[8] A. Neves, J. Romildo, D. Toledo, and F. Jo, "A study of CO 2 capture by high initial strength Portland cement pastes at early curing stages by new non-conventional thermogravimetry and non-conventional differential thermal analysis," J. Therm. Anal. Calorim., 2017.

[9] S. Ghabezloo, J. Sulem, and J. Saint-marc, "Evaluation of a permeability-porosity relationship in a low permeability creeping material using a single transient test," vol. 46, pp. 761–768, 2009.

[10] S. Bahafid, S. Ghabezloo, M. Duc, P. Faure, J. Sulem, "Cement and Concrete Research Effect of the hydration temperature on the microstructure of Class G cement : C-S-H composition and density," Cem. Concr. Res., vol. 95, pp. 270–281, 2017.

[11] J. Sercombe and C. Galle, "Rehydration and microstructure of cement paste after heating at temperatures up to 300 ° C," vol. 33, pp. 1047–1056, 2003.

[12] E. B. Nelson et al., "Well Cementing," 1990.

[13] M. Mainguy and M. M. Mod, "Mod eles de diffusion non linéaire en milieux poreux . Applications a la dissolution et au s'echage des materiaux cimentaires," 1999.

[14] B. Huet, V. Tasoti, and I. Khalfallah, "Energy Procedia A review of Portland cement carbonation mechanisms in CO 2 rich environment .," Energy Procedia, vol. 4, pp. 5275–5282, 2011.

[15] S. Ghabezloo, "Cement and Concrete Research Effect of the variations of clinker composition on the poroelastic properties of hardened class G cement paste," Cem. Concr. Res., vol. 41, no. 8, 2011.

[16] S. Ghabezloo, "Comportement thermo-poro-mécanique d ' un ciment pétrolier," 2009.

[17] Patrick Dangla, & Arnaud Bonnard. (2017, October 31). Ifsttar/bil: first version in github (Version v2.4). Zenodo. http://doi.org/10.5281/zenodo.1039729